Heat Capacity of Gadolinium near the Curie Point*†

Edwin A. S. Lewis‡
Department of Physics and Materials Research Laboratory, University of Illinois, Urbana, Illinois 61801
(Received 10 November 1969)

The dependence of the heat capacity of gadolinium on temperature has been observed close to the ferromagnetic Curie point at about 18 °C. An "ac" or temperature-modulation method allowed the use of very small single-crystal samples. The heat-capacity peak for our best sample is rounded in a range of $\frac{1}{2}$° at the Curie point (T_C). Outside this region, good power-law fits are obtained for a range of values of the critical exponents α (above T_C) and α' (below T_C), the choice of which depends on the choice of T_C. The entire set of data, including those in the rounded region, fits an expression derived from a simple macroscopic model of rounding. The T_C specified by this fit makes $\alpha = -0.09 + 0.05$ and $\alpha' = -0.32 \pm 0.05$. Tables of recent theoretical and experimental results are included for comparison. Our results on Curie point and rounding are in disagreement with recent conjectures of Cadieu and Douglass for gadolinium.

I. INTRODUCTION

In the last few years, widespread interest in the behavior of materials near critical points has stimulated a lengthening list of experiments[1,2] and calculations.[3] The critical behavior of a real system often is found to resemble closely that of an Ising or Heisenberg model, as determined by high- or low-temperature expansion methods. Still to be answered, however, is the question: Which details of a model must be adjusted to correspond with features of a given material, in order to predict the critical behavior? The dimensionality of the system is known to be crucial, and the anisotropy of the interaction is thought to be also, e.g., Ising and Heisenberg models behave differently. Recent calculations for classical (spin-∞) magnets have covered more fully the effects of this anisotropy.[4-6] It is usually thought, also, that spin is important in magnets. These may be the *only* important details for the "ideal" behavior in which the transition is not rounded.

Further careful experiments are necessary for comparison of critical behavior in materials which differ from each other in various ways, including the above. The "scaling laws"[7] which relate the behavior of various properties near the critical point also require further comparison with experiment through the measurement of various quantities in the same material. Finally, the causes of rounding of theoretically sharp peaks or discontinuities at the critical point are not clear.

We have measured the temperature variation of the heat capacity of gadolinium in zero applied field, in the vicinity of its ferromagnetic Curie point (T_C) at about 18 °C. Gadolinium[8] is a rare-earth metal in which the unpaired magnetic electrons are localized in the 4*f* shell. Interaction between ions is through indirect exchange, by means of conduction electrons. Unlike the other rare earths, gadolinium has low magnetic anisotropy, comparable to that of nickel and iron. Spin-wave experiments show that "gadolinium behaves like a classical Heisenberg ferromagnet"[8] at low temperatures. The saturation moment per atom is $7.55\mu_B$, close to the spin $\frac{7}{2}$ predicted by Hund's rule for the ground state. In comparison with various theoretical results and with other experiments, gadolinium may give us useful information on the importance of magnetic anisotropy; how important spin is in critical behavior; whether the hexagonal lattice structure makes any difference.

We are looking for the critical indexes α and α' in the power laws

$$C_H = A\epsilon^{-\alpha} + B, \qquad T > T_C,$$
$$\text{and} \quad C_H = A'\epsilon^{-\alpha'} + B', \quad T < T_C, \tag{1}$$

where $\epsilon = |(T - T_C)/T_C|$, and T_C, α, α', A, A', B, and B' are unknown constants. This form of expression has been found to fit predictions for Ising and Heisenberg models quite well. In the limit when $\alpha \to 0$,

$$C_H = -a \ln\epsilon + b, \tag{2}$$

where $A/\alpha \to a$, and similarly for $\alpha' \to 0$, where $A'/\alpha' \to a'$.

Section II proceeds to describe the experiment. In Sec. III the analysis of data is discussed. We compare our data with power laws, and also with a rounded curve given by a simple expression which assumes random variation of T_C throughout the sample. In Sec. IV we present tables of recent results for α and α', from calculation and from experiment, and compare with our best values. The disagreement between our observations of rounding and recent predictions for it are also discussed. Our corrected relative heat-capacity

data is recorded in the Appendix.

II. EXPERIMENT

A. Apparatus and Procedure

We use a version of the "ac" method originally introduced by Kraftmakher[9] and Sullivan and Seidel[10] and recently applied at high temperatures by Handler, Mapother, and Rayl[11] to measure the heat capacity of nickel. The sample is attached to a copper heat sink by means of a thin "heat leak." Light pulses strike the sample, causing its temperature to oscillate at a low frequency; the amplitude of this temperature modulation, measured by a small thermocouple junction attached to the sample, is inversely proportional to the heat capacity.

Figure 1 shows the sample-heat sink assembly. The copper heat sink is $\frac{1}{2}$ in. in diameter. It is suspended in vacuum, in a can which is immersed in an ice bath. The (approximately) $80\times60\times5$ mil blackened gadolinium sample, the matching piece of copper foil, and the thin aluminum foil heat-leak strip form a sandwich, held together by apiezon H grease, which moves up and down uniformly in temperature. One mil copper and constantan thermocouple wires are spot welded to this copper foil, rather than the gadolinium itself, in order not to cause any nonuniformity in temperature across the sample. The copper foil also helps to even out the temperature across the long dimensions of the sample. Apiezon H grease was chosen for its uniform properties over a large range of temperature; silicon grease had a strong tendency to creep over the sample. The ends of the aluminum foil strip are greased to the heat sink with a thin layer of Mylar in between for electrical insulation.

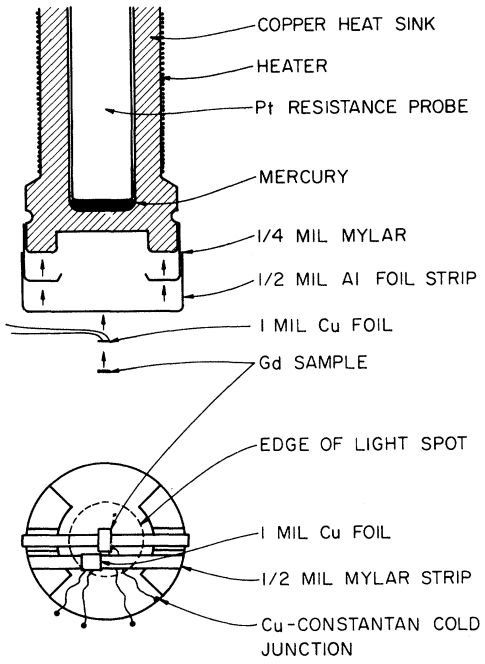

FIG. 1. Sample heat sink assembly.

The emf at 4 cps produced by this thermocouple is typically about 120 nV rms, corresponding to a rms temperature modulation of 3 mdeg. This signal is fed into a Princeton Applied Research (PAR) HR-8 lock-in amplifier with type B preamplifier, and the resulting dc output appears on a chart recorder. The data finally consist of a series of relative specific-heat values at well-defined temperatures.

The temperature of the heat sink is measured and controlled within a tolerance of about 1 mdeg, by a PAR PT-2 thermometer, whose platinum resistance is within a probe inserted into the heat sink as shown. (Absolute temperatures are known to ±0.2 °K from a rough calibration.) To reduce possible thermal gradients within the heat sink, a second small heat sink is located along the stainless-steel tube connecting it to the outside of the vacuum system. This second piece is controlled to about a tenth of a degree, using a thermistor, about 1 deg below the temperature of the main heat sink. Thus, the power required to heat the main sink is small, and does not vary much with the temperature of operation. Both heaters operate with ac at about 10 kc in order to avoid producing any magnetic field at the sample.

The temperature difference between the sample and the sink is measured using the same thermocouple that measures the ac temperature amplitude. The cold junction of the copper-constantan thermocouple is soldered directly to the sink; periodically its dc voltage is measured using a Leeds and Northrup K-5 potentiometer, giving the temperature difference to within a hundredth of a degree. This represents the tolerance for relative temperature measurements.

A small focused bulb, whose lens has been sanded to produce a uniform beam, shines upward from the bottom of the vacuum can and produces the light spot shown in Fig. 1. The amplitude of the 4-cps square-wave voltage applied to the filament is controlled as follows: A separate blackened piece of Cu foil, shown in the bottom view in Fig. 1, is suspended near the sample, with additional Cu and constantan wires spot welded to it. The ac signal produced by this sensor is fed into a second lock-in, and the resulting dc voltage is used to regulate the bulb voltage. Periodically this second ac signal is measured with the HR-8. In analysis the data are corrected accordingly, to represent temperature modulation at constant heating

amplitude. The bulb still, however, is the principal source of random noise, which is about 0.002 of the signal.

The corrected signal thus varies as the ratio of the heat capacity of the copper sensor to that of the sample. In analysis, this signal is multiplied by $1 - 0.000\,66T$ (T in °C) [12] to compensate for the changing heat capacity of copper.

B. Temperature Modulation Method: Checks on Accuracy

When heat is supplied at a rate $Q = Q_0 e^{i\omega t}$, the temperature measured at the point where the sample is attached to the heat-leak strip is $T = T_{DC} + T_0 e^{i(\omega t - \phi)}$ where, to lowest order in ω, and in the limit that the internal thermal relaxation of the heat-leak strip is much faster than the heating modulation, [10]

$$T_0 = \frac{Q_0}{\omega C_s}\left(1 + \frac{\omega^2\tau_s^2}{90} + \frac{1}{\omega^2\tau_e^2} + \frac{2K_l}{3K_s}\right)^{-1/2}$$

and $$\phi = \frac{\pi}{2} + \tan^{-1}\left(\frac{\omega\tau_s}{6} - \frac{1}{\omega\tau_e}\right), \qquad (3)$$

with $$\tau_s = \frac{L_s^2}{D_s}, \quad \tau_e = \frac{C_s}{K_l}, \quad D_s = \frac{k_s}{c_s\rho_s}.$$

Here subscripts s and l refer to sample and heat leak. The c and k are gram specific heat and thermal conductivity, while C, K, L, A, and ρ are, respectively, total heat capacity, thermal conductance, length in the direction of heat flow, cross section normal to the heat flow, and density. The τ_s represents an internal sample relaxation time which must $\ll 1/\omega$; the τ_e is the time constant for relaxation to the sink which must $\gg 1/\omega$. (Throughout this section "sample" will refer to our Gd-Cu-grease-Al sandwich.)

One may still do the experiment if the thermal relaxation internal to the heat leak does not keep up with the temperature modulation of the sample. In the slow internal-leak-relaxation limit, [13]

$$T_0 = \frac{Q_0}{\omega C_s}\left[1 + \frac{\omega^2\tau_s^2}{90} + \left(\frac{2}{\omega\tau_e'}\right)^{1/2} + \frac{1}{\omega\tau_e'} + \frac{K_l}{3K_s}\left(\frac{2\omega C_l}{K_l}\right)^{1/2}\right]^{-1/2}$$

and $$\phi = \tan^{-1}[1 + (2\omega\tau_e')^{1/2}] + \tan^{-1}\tfrac{1}{6}\omega\tau_s, \qquad (4)$$

where $$\tau_e' = \tau_e(C_s/C_l).$$

To check that $\omega^2\tau_s^2/90$ is very small, we measured the phase shift up to high frequencies using a CdS cell to detect the light modulation. The phase shift is $90° \pm 5°$ from 1.5 cps (the lower limit of the lock-in) to about 19 cps. Assuming that the leak-relaxation times are long, this is a sensitive indication that at 4 cps no correction for τ_s is needed.

Our estimates indeed put us in the limit $\tau_s \ll 1/\omega$ at 4 cps, and close to the situation represented by (4), with L_l about twice as long as the leak "thermal length" which can follow the temperature modulation. We measured the time τ_e by actually looking at the sample thermocouple emf as heating is turned off, using a Keithley 149 millimicrovoltmeter, and found τ_e to be 5 sec. Since C_s/C_l is about 3, we get $1/\omega\tau_e' = \frac{1}{375}$. The term $(2/\omega\tau_e')^{1/2}$ is small and is inversely proportional to C_s, so it provides only a small constant correction to the experimentally determined heat capacity and can be ignored. The fourth correction term is small and independent of C_s. Thus, the sample heat capacity is as close as desired to the inverse of the signal observed.

C. Sample Preparation

Most of our data were obtained on samples cut from a crystal made by the Aremco Corp. from material supplied by the Lunex Co. A mass spectrographic analysis at the Materials Research Laboratory facility showed about 0.1% rare-earth impurities and about 0.5% other impurities. Rectangular pieces about $80 \times 60 \times 20$ mils were spark cut and mechanically polished to 5 mils thick. They were annealed for 8 h at 1100 °C.

Sample X, for which the most data will be presented, was cut such that the c axis would be perpendicular to the long dimensions. Laue x-ray photographs show that the c axis is 5° from this direction; the spots are sharp. Its resistance ratio is $\rho(295\,°\text{K})/\rho(4\,°\text{K}) = 19$.

Sample Y, included for comparison, was blackened and probably contaminated during the annealing process. The c axis is, within 1°, parallel to the faces of largest area, and is 7° from parallel to the longest edge. Its resistance ratio is 9.

III. DATA ANALYSIS AND RESULTS

A. Corrections to Raw Data

The inverse of the signal (after the corrections for bulb brightness and the varying heat capacity of the Cu light sensor) is proportional to

$$C_{\text{tot}} = C_{\text{mag}} + C_l + C_e + C_{\text{Cu}} + C_{\text{Al}} + C_{\text{gr}}, \qquad (5)$$

the sum of the gadolinium magnetic, lattice, and electronic heat capacities, and those of the copper foil, the aluminum foil, and grease, respectively, in the sandwich. Before fitting to find the exponents α and α' in (1), we correct by subtracting the temperature-varying parts of the other heat capacities, to the necessary accuracy.

We estimate the contribution of the Cu and Al from the relative volumes in the sandwich. The

data are also compared with that of Griffel, Skochdopole, and Spedding[14] for the heat capacity of gadolinium over a wide range. A rough fit gives a check on the relative value of $(C_{Cu}+C_{Al}+C_{gr})$, indicating that C_{gr} may be neglected. C_l and C_e may also be estimated from the calculations in Ref. 14. We find that the effect of $C_l+C_e+C_{Cu}+C_{Al}+C_{gr}$ may be adequately compensated for by using $(C_{tot}-Tx)$ for further fits, where x is about $0.0005\ C_{tot}(30\,^\circ\mathrm{C.})$.

Thermal expansion causes the exchange energy to change, so to compare with the models discussed above, $C_{v,H}$ must be determined from the measured $C_{p,H}$. The well-known expression $C_p - C_v = TV\beta^2/K_T$, where β and K_T are the volume thermal expansion and volume isothermal compressibility, may be used together with the Pippard relations[15] for a second-order transition; $C_p = TV\xi\beta + K_1$ and $K_T = \beta/\xi + K_2$ where $\xi = (dP/dT)_\lambda$, the slope of the "lambda line," or the pressure dependence of the Curie point, and K_1 and K_2 are constants. We obtain the value of K_1 by comparing our data and that of Ref. 14 with the thermal-expansion data of Cadieu and Douglass.[16] ξ has been measured by Robinson, Milstein, and Jayaraman.[17]

From the values of β found by Cadieu and Douglass, however, $|\beta|/\xi$ is always $\ll K_T(25\,^\circ\mathrm{C})$, which is the tabulated compressibility. Thus β/ξ may be ignored; K_T does not vary significantly in the transition region. With this approximation, from the above,

$$C_v = C_p - (C_p - K_1)^2/TV\xi^2K_T\ . \tag{6}$$

This is a significant correction in absolute terms (several percent at the peak), but is not so important for the form of the function. Suppose $C_p = A_p\epsilon^{-\alpha} + B_p$, then (6) leads to

$$C_v = A\epsilon^{-\alpha} + B\ ,$$

where
$$A = A_p + (A_p/x)(2K_1 - 2B_p - A_p\epsilon^{-\alpha}) \tag{7}$$

and
$$B = B_p + (1/x)(2B_pK_1 - B_p^2 - K_1^2)\ , \tag{8}$$

with $x = TV\xi^2K_T$. The corrections may be found using the known value of K_1 and the A_p, B_p, and α from our fits. We conclude that there is not enough difference in the temperature dependence of C_p and C_v to require correction. Thus T_C, α, and α' may be found directly from a fit of the C_p data.

The true C_v curve might itself be distorted due to a lattice contraction, in that each measurement of C_v at a new temperature is made with a new lattice constant and thus a different J. The system sees a different T_c at each point. We investigated the effect of expressing $C = A\epsilon_v^{-\alpha} + B$ in terms of ϵ_p, where $\epsilon_v = \epsilon_p + \Delta\epsilon(T)$, with the aid of the above-mentioned data and from the Pippard point of view. Again, however, the difference between curves with lattice contraction allowed, and not allowed, is well within the noise in the region used for the power-law fit.

B. Power-Law Fit

The whole range of measurements for sample X, which produced the sharpest transition, is presented in Fig. 2. The numerical data corresponding to these points may be found in the Appendix.

The analysis was suggested by Van der Hoeven, Teaney, and Moruzzi.[18] It is assumed that $C = A\epsilon^{-\alpha} + B$, i.e., that C is a linear function of the quantity $\epsilon^{-\alpha}$. Given a set of data points $C_i(T_i)$ (either above or below T_C) and a specified T_C and α, only algebra is needed to fit a straight line to the function $C(\epsilon^{-\alpha})$, i.e., to find A and B. Then $\chi^2(T_C, \alpha)$ is calculated

$$\chi^2(T_C, \alpha) = \sum_{i=1}^{N} \frac{[A\epsilon^{-\alpha} + B - C_i(T_i)]^2}{(\Delta C_i)^2}\ , \tag{9}$$

where N is the number of data points and ΔC_i is the estimated random noise in measurement. The computer prints χ^2 for each of a large number of combinations of T_C and α. We require the values T_C and α, which give the minimum value of χ^2, and the range over which an acceptable fit is possible.

The heat-capacity curves clearly departed from the pure singular behavior in regions of width about $\frac{1}{2}\,^\circ$C for sample X and $1\frac{1}{2}\,^\circ$C for sample Y. Only points outside these regions were used for power-law fits; if points too close to T_C were fed into the analysis, no good fit to a power law was found. Data at very high and very low temperatures were not used for the fit, on the assumption that critical behavior is not likely to extend indefinitely far away from T_C. (The idea of the critical region is discussed in Ref. 2.) This made little difference to the fit, however, as can be seen in the log-log plots.

On each side of the transition, using data approximately in the range $10^{-3} < \epsilon < 5\times10^{-2}$, good fits are possible over a sizable range of α's, depending on which T_C is chosen. Figure 3 summarizes the information on T_C, α, and α' obtained from sample X. For each data set (above or below T_C) the large dot locates the minimum in χ^2. The solid line indicates the α(or α') which minimizes χ^2, for any given T_C. The dashed line is a line of constant χ^2, arrived at by interpolating in the table of $\chi^2(T_C, \alpha)$ mentioned above. Roughly, we estimate at least a 90% probability that the "true" combination of T_C and α(or α') lies within the dashed boundary. This estimate was arrived at by a rough integration

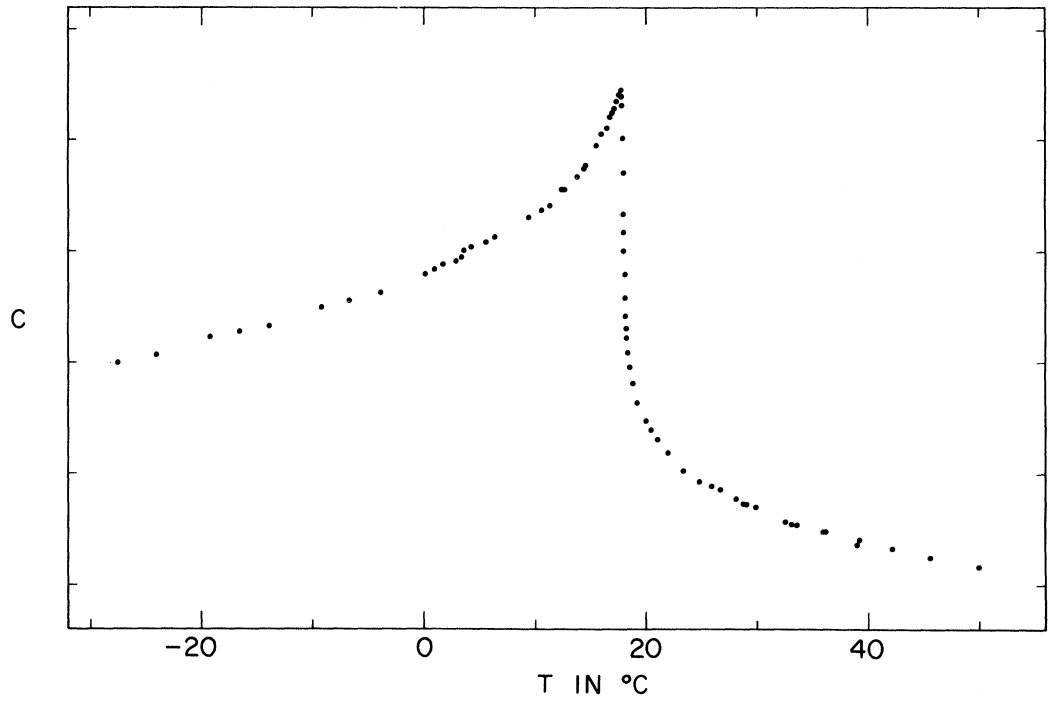

FIG. 2. Temperature variation of the magnetic heat capacity: the full range of data for sample X.

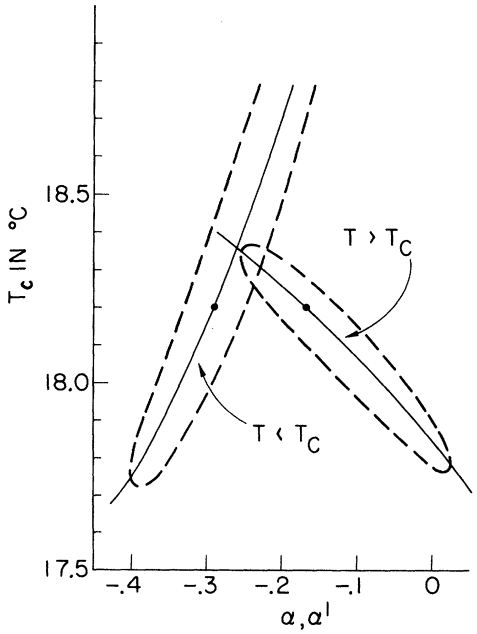

FIG. 3. Results of power-law fits for sample X. The large dots locate the χ^2 minima, for $T > T_C$ and $T < T_C$, in the (T_C, α) or (T_C, α') plane. The solid lines indicate α for minimum χ^2, for any given choice of T_C. The probability of the "true" (T_C, α) lying within the dashed boundary (or its extension) is about 0.9, given our data.

of the likelihood function $L(T_C, \alpha) \sim \exp(-\frac{1}{2}\chi^2)$ over areas in the (T_C, α) plane.

For sample X, the above and below data agree on a best Curie temperature of 18.2 °C, with $\alpha = -0.17$ and $\alpha' = -0.29$. The log-log plots in Fig. 4 demonstrate fits close to these. For comparison, Fig. 5 presents plots for $T_C = 18.05$ °C, the temperature necessary to fit the expression below for a rounded curve.

We plotted $[A\epsilon^{-\alpha} + B - C(T)]$, the deviation of data from the theoretical formula, for each of many combinations of T_C and α, with A and B given by the computer fit. The best-looking plots, i.e., those which, to the eye, showed the least systematic deviation, were also the ones corresponding to the plots of Fig. 4, the closest to the minimum in χ^2.

C. Fit to Rounded Curve

Consider the magnet as made up of many regions, each with a different Curie point.[19] (It is known that the Curie point is rather sensitive to such variables as impurity content and pressure, and, in fact, it is hard to find two samples of the same material with the same Curie point.[20]) Suppose that the heat capacity of the completely homogeneous material within each region is

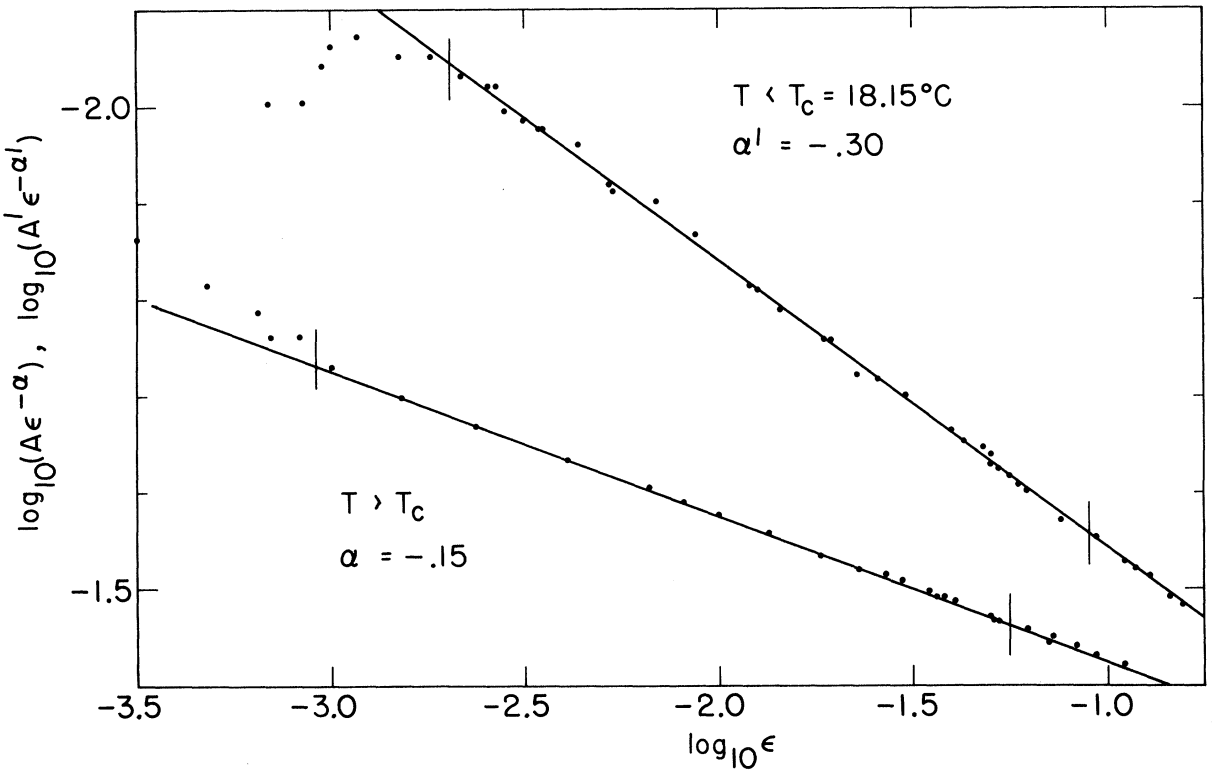

FIG. 4. Log-log plots for sample X, using approximately the parameters T_C, $A(A')$, and $B(B')$ which give the overall best power-law fit above (below) T_C. Thus, each point represents $\log_{10}[C(T)-B]=\log_{10}(A\epsilon^{-\alpha})$ for a given datum $C(T)$ above T_C, etc. The short vertical lines define the data used in each power-law fit. The straight lines represent ideal power-law behavior for the given α or α'.

$$C_{\text{hom}}(T, T_C) = A\epsilon^{-\alpha} + B, \quad T > T_C$$
$$= A'\epsilon^{-\alpha'} + B', \quad T \leq T_C \ . \tag{10}$$

Further, suppose that the distribution of T_C among the regions is Gaussian, centered on T_{C0}, with a half-width d. Then the heat capacity of the whole crystal is

$$C = K\int_{-\infty}^{\infty} C_{\text{hom}}(T, T_C)\exp\left(-\frac{(T_C - T_{C0})^2}{2d^2}\right)dT_C \ . \tag{11}$$

We compare our data with this expression.

The computer was asked to calculate a theoretical $C(T)$ according to (11), for each of a set of temperatures T at which an experimental C had been found. This was done for each of a number of combinations of T_{C0} and d. Given T_{C0}, the parameters A, A', α, α', B, and B' were fed in which had given the minimum χ^2, with T_{C0} as the Curie point, in the power-law fit. (The normalization factor K was computed to minimize χ^2 once the integration had been done.) $\chi^2(T_{C0}, d)$ was calculated and a plot of deviations of the data from (11) was made.

No set search program was used. The fit is very sensitive to T_{C0} and d, however, so not many trials were required to find the best (T_{C0}, d) to the nearest 0.01° in both parameters. This is shown in Fig. 6, for sample X. $T_{C0}=18.05\,^\circ$C, $d=0.15\,^\circ$C, $\alpha=-0.1$, and $\alpha'=-0.3$ for this curve. Figure 7 displays the fit for sample Y, with $T_{C0}=18.08\,^\circ$C, $d=0.55^\circ$, $\alpha=-0.05$, and $\alpha'=-0.2$.

IV. DISCUSSION

For comparison with Ising and Heisenberg models, Table I lists a number of recent theoretical results for α and α'.

Figure 3 shows that a wide range of values for α is allowed, depending on the T_C chosen. The predictions of -0.2 for the spin-$\frac{1}{2}$ Heisenberg model and of -0.1 or -0.07 for the classical or spin-∞ Heisenberg model are all well within this range.

Encouraged by the success of the fit to the rounded curve, however, we will assume that the inhomogeneity conjecture which led to Eq. (11) is correct. Then T_C is pinned down to $18.05\pm0.02\,^\circ$C for sample X, and α is restricted to -0.09 ± 0.05. This is in agreement with the prediction for the spin-∞ Heisenberg model. It seems reasonable

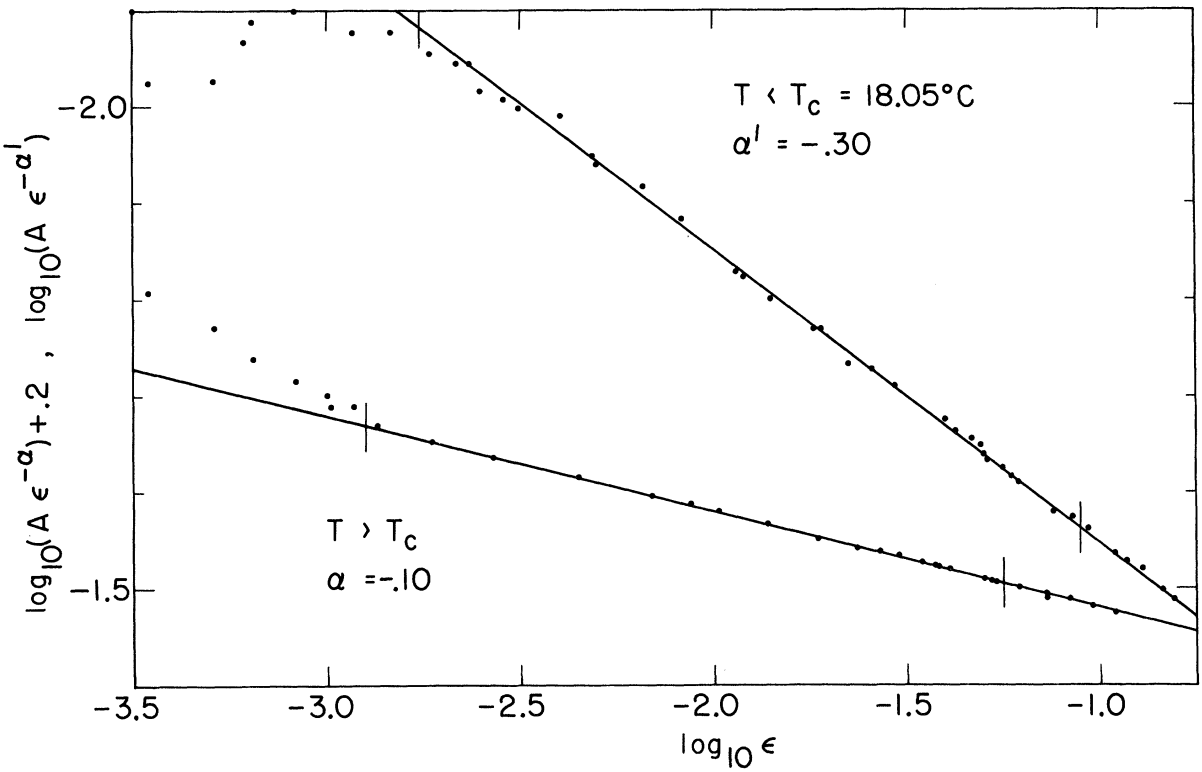

FIG. 5. Log-log plots for sample X using the parameters T_C, $A(A')$, and $B(B')$ used for the "rounded fit". The short vertical lines define the data used in each power-law fit. The straight lines represent ideal power-law behavior for the given α or α'.

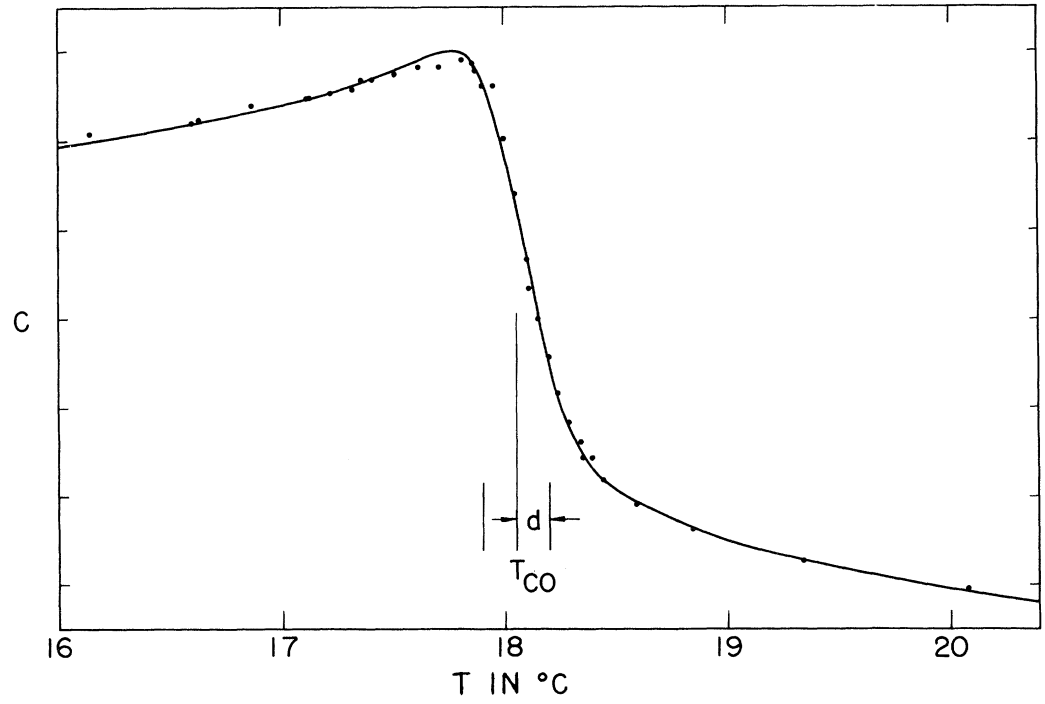

FIG. 6. Experimental points for sample X compared with curve calculated from Eq. (11), using parameters $T_{C0} = 18.05\,^{\circ}\mathrm{C}$, $d = 0.15\,^{\circ}\mathrm{C}$, $\alpha = -0.1$, and $\alpha' = -0.3$. The values of A, A', B, and B' are those which give the best power law fits for $T_C = T_{C0}$ and this α and α'.

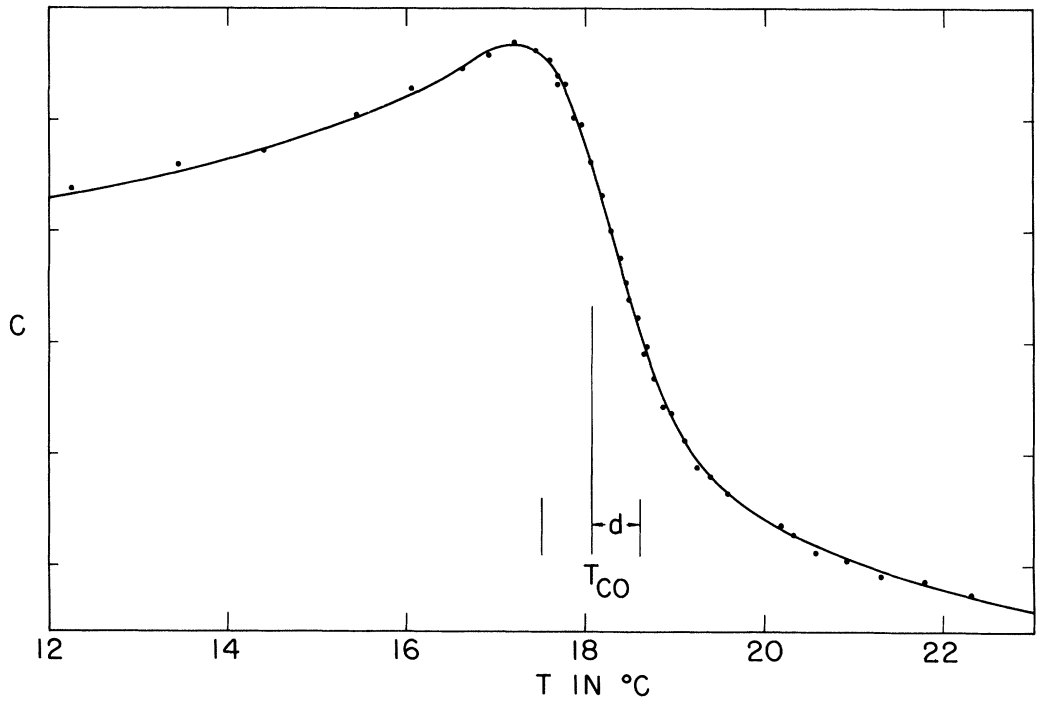

FIG. 7. Experimental points for sample Y compared with curve calculated from Eq. (11), using parameters $T_{C0} = 18.08\,^{\circ}\mathrm{C}$, $d = 0.55\,^{\circ}\mathrm{C}$, $\alpha = -0.05$, and $\alpha' = -0.2$. The values of A, A', B, and B' are those which give the best power-law fits for $T_C = T_{C0}$ and this α and α'.

that a spin-$\frac{7}{2}$ Heisenberg ferromagnet might behave more like the spin-∞ case than the spin $\frac{1}{2}$.

This choice of T_C makes $\alpha' = -0.32 \pm 0.05$. We know of no theoretical predictions for α' for a Heisenberg model; there may be a parallel in the Ising model results of Table I which indicate that α' is probably more negative than α, at least if one looks at $\epsilon > 10^{-4}$.

It is unlikely, but possible, that our results are consistent with the scaling law $\alpha = \alpha'$,[2] referring to Fig. 3.

Table II compares these results for α and α' with those of several other recent measurements of critical magnetic heat capacities.

An interesting recent paper by Cadieu and Douglass[16] (CD) investigates the effect of impurity concentration on the Curie point and on rounding in gadolinium. Measurements of the thermal-expansion coefficient β (according to Pippard,[15] $C_p = TV\xi\beta + K_1$) are combined with previous heat-capacity results of Voronel.[21] Simple empirical formulas result for T_m and $\Delta T = T_i - T_m$ as a function of resistance ratio, where T_m and T_i are the temperatures for, respectively, the maximum C (or $|\beta|$) and the point of inflection on the high-temperature side of the heat-capacity curve. Neither T_m nor ΔT for our curves is in agreement with these relationships: The temperatures T_m for samples X, Y, and others are a degree or more too high, well outside our confidence limits for absolute-temperature measurement, and our ΔT's are too small by factors of 3 to 8. Nor was there any clear correlation between T_m and ΔT for a number of different samples.

The simple inhomogeneity model for rounding which is expressed by (11) allows each small region of the crystal to undergo an ideal transition; C or $dC/d\epsilon$ may indeed become infinite. If inhomogeneity does exist, the change in the fluctuation spectrum invoked by CD to account for impurity effects is not necessary to produce rounding. It at least appears that this change has not occurred at the distance from the Curie point which CD would predict, given our resistance ratios. In fact, the quality of the fits to (11) suggests that the rounding in samples X and Y still may be due to inhomogeneity.[22]

What might be the source of this inhomogeneity? Our results for a number of different samples do suggest that the purer the material, the less the rounding. Annealing makes a tremendous difference in sharpening the peak, suggesting that internal strains are quite important. But the full answer is still unclear.

TABLE I. Series predictions for heat capacity. The critical indexes γ, γ', β, and Δ are defined in Ref. 2.

Model	α	α'	Comment
Ising, spin $\frac{1}{2}$			
2 dimensions [a,b]	0	0	$\alpha = \alpha'$
3 dimensions fcc [c]	"positive, of order $\frac{1}{8}$"		
All lattices [d]	$\frac{1}{8}$	$\frac{1}{8}$	
All lattices [e]		$0.066\ ^{+0.16}_{-0.04}$	Derived from γ', β, as well as C_H series
Tetrahedral [f]		0	Behavior when $\epsilon > 10^{-4}$
Tetrahedral [f]		$\frac{1}{8}$	When $\epsilon < 10^{-4}$
Heisenberg Spin $\frac{1}{2}$ fcc [g]	-0.2 ± 0.05		$C/R = (T_C/T)^2[1.206 - 0.966(1 - T_C/T)^{0.2}]$ in range $0.7 \leq T_C/T \leq 0.96$
Spin $\frac{1}{2}$ fcc [g]	-0.2		From scaling law $\alpha = 2 - \Delta + \gamma$
Classical, several lattices [h]	-0.07		From $\alpha = 2 - \Delta + \gamma$
Classical fcc [i]	-0.1 ± 0.1		$\eta_z = \eta_x = \eta_y$ [§]
Classical XY fcc [i]	0 ± 0.1		$\eta_z < \eta_x = \eta_y$ [§]
Spin ∞ Ising fcc [i]	0.1 ± 0.1		$\eta_z > \eta_x = \eta_y$ [§] in Hamiltonian $\mathcal{H} = -\frac{1}{2kT}\sum_{ij\alpha}\eta_\alpha J S_{i\alpha}S_{j\alpha}$
Classical all lattices [j]	-0.07		
XY model, spin $\frac{1}{2}$ fcc [k]	-0.20 ± 0.20		$\mathcal{H} = -J\sum_{ij}(\sigma_{ix}\sigma_{jx} + \sigma_{iy}\sigma_{jy})$

[a] L. Onsager, Phys. Rev. 65, 117 (1944).
[b] D. C. Mattis, *The Theory of Magnetism* (Harper and Row, New York, 1965), Chap. 9.
[c] M. F. Sykes, J. L. Martin, and D. L. Hunter, Proc. Phys. Soc. (London) 91, 671 (1967).
[d] D. S. Gaunt, Proc. Phys. Soc. (London) 92, 150 (1967).
[e] G. A. Baker and D. S. Gaunt, Phys. Rev. 155, 545 (1967).
[f] D. S. Gaunt and C. Domb, J. Phys. Soc. Japan 1, 1038 (1968).
[g] G. A. Baker, Jr., H. E. Gilbert, J. Eve, and G. S. Rushbrooke, Phys. Rev. 164, 800 (1967).
[h] R. L. Stephenson and P. J. Wood, Phys. Rev. 173, 475 (1968).
[i] Reference 4.
[j] Reference 5.
[k] Reference 6.

TABLE II. Comparison with recent results.

Material	Description	α	α'
Gd	hcp ferromagnetic metal with small anisotropy	-0.09 ± 0.05	-0.32 ± 0.05
EuO [a]	Cubic ferromagnetic insulator	0	Negative
$RbMnF_3$ [b]	Cubic antiferromagnetic insulator	0	Negative
EuS [c]	Cubic ferromagnetic insulator	0 ± 0.03	-0.25 ± 0.03
MnF_2 [d]	Tetragonal antiferromagnetic insulator	0 to 0.1	0
Ni [e]	Cubic ferromagnetic metal	0.104 ± 0.05	-0.262 ± 0.06

[a] D. T. Teaney, Natl. Bur. Std. (U.S.) Misc. Publ. No. 273, 50 (1966).
[b] D. T. Teaney, V. L. Moruzzi, and B. E. Argyle, J. Appl. Phys. 37, 1122 (1966).
[c] Reference 18.
[d] Reference 20.
[e] W. E. Maher and W. D. McCormick, Phys. Rev. 183, 573 (1969).

ACKNOWLEDGMENTS

It is a pleasure to thank Dr. C. P. Slichter for his guidance throughout this project. Discussions of theory and experiment with members of his research group have been extremely helpful. We thank Dr. D. E. Mapother for the use of his equipment in preparing samples and thermocouples.

APPENDIX: TABLE OF DATA FOR SAMPLE X

C_X here represents the heat capacity of the gadolinium-copper-aluminum-grease sandwich, in arbitrary units. It has been corrected to eliminate the *temperature-varying* parts of the copper, aluminum, grease, and gadolinium lattice and electronic heat capacities by subtracting the quantity $0.005T$ (°C) from the original total C. Thus, to the best of our knowledge, the magnetic heat capacity C_p of gadolinium is xC_X+y, where x and y are unknown constants. See Table III.

TABLE III. Data for sample X.

T(°C)	C_X	T(°C)	C_X	T(°C)	C_X
−27.4	12.00	16.60	14.10	18.39	12.22
−23.9	12.06	16.63	14.12	18.44	12.09
−19.1	12.23	16.87	14.20	18.59	11.95
−16.4	12.28	17.12	14.24	18.84	11.80
−13.8	12.33	17.13	14.24	19.34	11.63
−9.1	12.50	17.22	14.26	20.08	11.47
−6.6	12.57	17.32	14.28	20.54	11.38
−3.8	12.61	17.36	14.34	21.06	11.30
0.2	12.79	17.41	14.34	22.04	11.18
1.0	12.82	17.51	14.37	23.43	11.02
1.8	12.88	17.62	14.41	24.85	10.92
3.0	12.91	17.71	14.41	25.9	10.88
3.4	12.95	17.81	14.45	26.8	10.85
3.7	13.00	17.86	14.43	28.2	10.77
4.3	13.04	17.87	14.39	28.8	10.72
5.6	13.08	17.90	14.31	29.1	10.72
6.4	13.13	17.95	14.31	29.9	10.69
9.43	13.30	18.00	14.01	32.6	10.56
10.62	13.37	18.05	13.70	33.2	10.54
11.53	13.40	18.10	13.33	33.6	10.53
12.52	13.55	18.11	13.17	36.0	10.47
12.74	13.55	18.15	13.00	36.2	10.47
13.97	13.66	18.20	12.79	39.2	10.40
14.51	13.74	18.24	12.58	39.0	10.35
14.68	13.76	18.29	12.42	42.2	10.32
15.65	13.94	18.34	12.31	45.6	10.24
16.14	14.04	18.35	12.22	50.0	10.16

*Research supported in part by the U.S. Atomic Energy Commission, under Contract No. AT(11-1)-1198.

†Based on a thesis submitted in partial fulfillment of the requirements for the degree of Doctor of Philosophy in Physics, in the Graduate College of the University of Illinois, 1969.

‡Present address: Department of Physics, Union College, Schenectady, N. Y. 12308.

[1]A review of the experimental literature as of 1967 is P. Heller, Rept. Progr. Phys. 30, 731 (1967).

[2]L. P. Kadanoff, W. Götze, D. Hamblen, R. Hecht, E. A. S. Lewis, V. V. Palciauskas, M. Rayl, J. Swift, D. Aspnes, and J. Kane, Rev. Mod. Phys. 39, 395 (1967), review theory and experiment for static properties.

[3]The theoretical situation is reviewed in M. E. Fisher, Rept. Progr. Phys. 30, 615 (1967).

[4]D. Jasnow and M. A. Moore, Phys. Rev. 176, 751 (1968).

[5]H. E. Stanley, J. Appl. Phys. 40, 1272 (1969).

[6]D. D. Betts and M. H. Lee, Phys. Rev. Letters 20, 1507 (1968).

[7]Reference 2 presents one approach and gives further references.

[8]R. J. Elliott, in *Magnetism*, edited by G. T. Rado and H. Suhl (Academic, New York, 1965), Vol. IIA.

[9]Y. A. Kraftmakher, Zh. Prikl. Mekhan. i Tekhn. Fiz. 5, 176 (1962).

[10]P. F. Sullivan and G. Seidel, Phys. Rev. 173, 679 (1968).

[11]P. Handler, D. E. Mapother, and M. Rayl, Phys. Rev. Letters 19, 356 (1967).

[12]*A Compendium of the Properties of Materials at Low Temperature (Phase I)*, edited by V. J. Johnson (Natl. Bur. Stds. Washington, D.C., 1960), Table 4.112-1.

[13]P. M. Schwartz, thesis, University of Illinois, 1969 (unpublished).

[14]M. Griffel, R. E. Skochdopole, and F. H. Spedding, Phys. Rev. 93, 657 (1954).

[15]A. B. Pippard, *The Elements of Classical Thermodynamics* (Cambridge U.P., Cambridge, England, 1957), p. 143.

[16]F. J. Cadieu and D. H. Douglass, Jr., Phys. Rev. Letters 21, 680 (1968).

[17]L. B. Robinson, F. Milstein, and A. Jayaraman, Phys. Rev. 134, A187 (1964).

[18]B. J. C. Van der Hoeven, D. T. Teaney, and V. L. Moruzzi, Phys. Rev. Letters 20, 719 (1968).

[19]This approach is suggested by T. Yamamoto, D. Tanimoto, Y. Yasuda, and K. Okada, in *Critical Phenomena, Proceedings of a Conference* (Natl. Bur. Stds. Misc. Publication No. 273, Washington, D.C., 1966), p. 86; M. Rayl, O. E. Vilches, and J. C. Wheatley, Phys. Rev. 165, 692 (1968), and others.

[20]D. T. Teaney, Phys. Rev. Letters 14, 898 (1965).

[21]A. V. Voronel, S. R. Graber, A. P. Simkina, and I. A. Charkina, Zh. Eksperim. i Teor. Phys. 49, 429 (1965) [Soviet Phys. JETP 22, 301 (1966)].

[22]This interpretation is supported by P. G. Watson, J. Phys. C 2, 948 (1969), who argues that "large scale inhomogeneities" will produce rounding while "small scale and randomly distributed" defects will still allow a sharp transition.